PHYSICAL REVIEW B VOLUME 24, NUMBER 8 15 OCTOBER 1981

Magnetoconductance and weak localization in silicon inversion layers

R. G. Wheeler
Department of Engineering and Applied Science, Yale University,
P.O. Box 2157, New Haven, Connecticut 06520
(Received 9 March 1981)

Large magnetoconductivities are observed on high-mobility Si inversion layers in the temperature range of 4 – 1 K at very small magnetic fields. With the use of current localization theory the inelastic scattering rate has been extracted from the data as a function of both temperature and electron surface density. Inelastic lengths of about 8×10^{-5} cm at 1 K have been derived from the results. Band-structure effects are observed in the localization phenomena at very high electron surface densities.

INTRODUCTION

Logarithmic increases in resistivity at low temperatures have been observed in thin films and silicon inversion layers.[1,2] These experimental results have been interpreted in light of recent localization theory and compared with the form established for two-dimensional systems by Abrahams, Anderson, Licciardello, and Ramakrishnan.[3] The salient theoretical result is that no true metallic regime exists in two dimensions, but the conductivity of such systems will exhibit a logarithmic signature no matter how weak the disorder. Experimental evidence based only upon resistivity increases has been deemed by some investigators to be insufficient to convincingly confirm localization theory in two dimensions.[4]

Subsequently, magnetic effects have been investigated theoretically.[5,6] Following Altshuler, Khmel'nitzkii, Larkin, and Lee,[5] the change in conductivity with temperature T and magnetic field H is written as

$$\delta\sigma(H,T)=+\sigma_N\left[\psi\left[\frac{1}{2}+\frac{\hbar}{4DeH\tau_{\rm in}}\right]-\psi\left[\frac{1}{2}+\frac{\hbar}{4DeH\tau_e}\right]\right] \qquad (1)$$

in mks units (see Appendix). Here ψ is the digamma function, D is the diffusivity, e is the electronic charge, $\hbar$ is Planck's constant, τ_e is the elastic scattering time, and $\tau_{\rm in}$ is the inelastic scattering time. It is assumed that $\tau_{\rm in}$ alone is a function of temperature. In the limit $H=0$, since $\psi(Z)\rightarrow \ln Z$ as $Z\rightarrow\infty$,

$$\delta\sigma(H=0,T)=-\sigma_N\ln\frac{\tau_{\rm in}}{\tau_e} \ . \qquad (2)$$

At a fixed temperature the change in conductivity with field is

$$\Delta\sigma(H,T_{\rm const})=\delta(H,T)-\delta(H=0,\ T)=\sigma_N\left[\psi\left[\frac{1}{2}+\frac{\hbar}{4DeH\tau_{\rm in}}\right]-\psi\left[\frac{1}{2}+\frac{\hbar}{4DeH\tau_e}\right]\right]+\sigma_N\ln\frac{\tau_{\rm in}}{\tau_e} \ . \qquad (3)$$

σ_N, here called the localization conductivity, is given theoretically by

$$\sigma_N=\frac{e^2}{\hbar}\frac{1}{4\pi^2}S \ , \qquad (4)$$

S is the spin and orbital degeneracies.[7] In Si inversion layers of [100] orientation $S=2$, thus $\sigma_N=1.235\times10^{-5}$ (ohm/□)$^{-1}$. Since $\tau_{\rm in}\sim T^{-n}$, an increasing resistance with decreasing temperature is observed, and at a fixed temperature an increasing conductivity with magnetic field is expected. Here the magnetic field acts to remove or cut off the localization resistance. The scale of the conductivity changes is given by σ_N. Magnetoconductivities have been reported on silicon inversion layers which have been cited as evidence for two-dimensional localization theory.[8] Predictions regarding the Hall coefficient have been included in the theoretical treatment. Here the data to date appear inconclusive.[9,10]

 ©1981 The American Physical Society

We report here on the measurement of $\Delta\sigma\,(H,T_{\text{const}})$ over the range of $1-4.2$ K on high mobility [100] oriented silicon inversion layers. We find on the scale of σ_N, since

$$\sigma_N/\sigma \sim 1.235\times10^{-5}/3.7\times10^{-3} \sim 3\times10^{-3} \ ,$$

large conductivity increases with magnetic fields to 130 G, increases which at 1.27 K cancel resistance increases associated with ~ 2 decades in temperature. We have analyzed the data in light of Eq. (1) to extract the inelastic scattering time as a function of temperature and electron density n_s. We believe these results lend credence to the localization theory and at the same time supply new insights into the nature of the silicon inversion layers.

EXPERIMENTAL PROCEDURES

For magnetoconductance measurements sample configuration is of great concern due to the shorting effect of end contacts which introduce a $\Delta R/R$. This "Hall resistance" behaves very much like a true transverse magnetoresistance proportional to H^2 for small fields. Following Wick[11] and Drabble and Wolfe,[12] we have designed four terminal geometries where λ/ω, the ratio of the probe-to-end-contact distance λ to the channel width ω, is greater than 5. This assures us that any fictitious $\Delta\rho/\rho$ is $<10^{-6}$ for fields less than 130 G and mobilities of $\sim 20\,000$ cm^2/V sec. Thus we measure changes in $\rho_{xx}(H)$ without corrections to the above order. A normal magnetoresistance is also expected. If we assume that its magnitude can be predicted by the classical solution to the Boltzmann equation for most of the results reported here, the error associated with the assumption that $(\sigma_{xx})=(1/\rho_{xx})$ is significantly less than other errors.[13]

The samples fabricated on ~ 25 ohm cm p-type silicon substrates have maximum mobilities of $\sim 16\,000$ cm^2/V sec at 4.2 K and an oxide fixed charge density, $Q_{ss}\sim 8\times10^{10}$ cm^2. The sample geometries and oxide capacitance were measured to better than 1%. These characteristics are displayed in Table I. The devices were mounted on headers fabricated from Teflon and phosphor bronze. Gold wire bonding was employed. Initial results, not to be included in the subsequent discussion, on devices mounted on normal Kovar headers were subjected to a very troublesome magnetic hysteresis associated with Kovar. All soldering of leads was done with a very minimum of tin-lead solder at least 3 cm away from the device to preclude magnetic field distortions due to superconducting materials.[14] The devices were immersed in liquid helium together with a germanium resistance thermometer within an electrostatic shield. The resistance thermometer was not magnetic field sensitive in the fields used. The field was generated with a solenoid immersed in the liquid nitrogen dewar. This solenoid was wound with a single layer of copper wire with 1312 turns per meter over a length of 27.5 cm. The coil diameter of 4.48 cm assured us that the geometry correction is less than 1.5%. The current was measured with a precision Leeds and Northrop-type 4361 shunt, providing an accuracy in the magnetic field determination of 1%.

The conductivity measurements were performed in two ways. $\Delta\sigma(H=0,T)$ was measured with a double bridge, the detector was a PAR 126 lock-in amplifier with a sensitivity using an output amplifier of $\sim 3\times10^{-9}$ V, operating at 27 Hz. Using measuring fields of less than 1.0 mV/cm, one obtained reproducibility in the bridge settings of ± 0.2 ohm. $\Delta\sigma(H,T_{\text{const}})$ were measured by two methods. The bridge out-of-balance voltage was recorded as the magnetic field was applied, whereupon calibration was obtained by two bridge balances, at

TABLE I. MOSFET device characteristics.

	AB20	TB10
Source-drain length (mm)	2.491 ± 0.01	2.501 ± 0.01
Gate width (mm)	0.0987 ± 0.001	0.1034 ± 0.001
Mean probe separation (mm)	1.170 ± 0.01	1.174 ± 0.01
Probe width (mm)	0.019 ± 0.001	0.017 ± 0.001
Total area (mm^2)	0.2544	0.2586
Oxide capacitance (μF)	115.9 ± 1.0	92.8 ± 1.0
Maximum mobility (cm^2/V sec)	$\sim 16\,000$	$\sim 17\,000$
Q_{ss} (cm^{-2})	$\sim 5\times10^{10}$	$\sim 5\times10^{10}$

$H=0$ and $H=130$ G. This tedious method was replaced by a constant current source at 27 Hz of $i=0.285\times10^{-7}$ A; the voltage difference between probes was balanced by the internal lock-in offset, whereupon the $\Delta\sigma(H)$ was recorded as the field was increased. These two methods gave exactly the same results. Most of the data reported here involved the latter for the $\Delta\sigma(H)$ determinations.

In order to ascertain that non-Ohmic behavior did not exist in the measurement[2] using the latter method, i was increased and decreased by a factor of 10, i.e., a range of 100 in the electric field. Only at the highest value was a small but perceptible change in the magnetoconductance observed. Electrostatic equilibrium of the depletion layer of the device was obtained initially by the application of a -3.0-V bias to the substrate and a small gate voltage at 77 K. During cycling of the device numerous times to 4.2 K the channel resistance at any given gate voltage has remained stable to 1 part in 3000. The gate voltage stability and reproducibility is about 1 part in 10^6.

EXPERIMENTAL RESULTS AND ERRORS

Conductivity changes may be caused by both localization and a temperature-dependent elastic scattering.[15,16] Owing to this latter effect, caused by Coulomb and surface-roughness scattering, one cannot convincingly separate from conductivity measurements that part which is characterized by a $\ln T$ dependence with T ranging from 4.2 to 1 K. Data (not to be displayed here) consistently yielded slopes of σ_N to 1.6 σ_N dependent upon n_s and device quality.

In what follows we assume that the magnetoconductance is solely due to localization and can be described by Eq. (3). Although other temperature-dependent processes clearly occur, no others except the localization model seem to be able to account for a magnetoconductance of the magnitude observed.

A sample of the magnetoconductance at electron surface density of 6.85×10^{12} cm^{-2} is shown in Fig. 1. The striking result at 1.27 K is that $\Delta\sigma/\sigma_N\approx1$ occurs at about 40 G; the field cancels out the localization resistance caused by a decade change in temperature.

In order to compare the data with the theory, the following procedure was adopted. Only τ_{in} is to be allowed to vary. The diffusivity is given by

$$D=\tfrac{1}{2}v_F^2\tau_e=\sigma/\rho_D e^2 \ , \tag{5}$$

for a two-dimensional Fermi gas. Here v_F is the Fermi velocity and ρ_D is the electron density of states associated with the [001] orientation. $\rho_D=2m^*/\pi\hbar^2$ where we use $m^*=0.19m_e$. The elastic time $\tau_e=\sigma m^*/n_s e^2$ is determined from the conductivity and the electron surface charge density n_s. For a particular electron density n_s and the corresponding σ we now calculate $\Delta\sigma(H,a)$ for a fixed magnetic field H_1 as a function of $a=\tau_{in}/\tau_e$. From plots of such calculations the values of a are determined using the measured $\Delta\sigma(H_1,T)/\sigma_N$

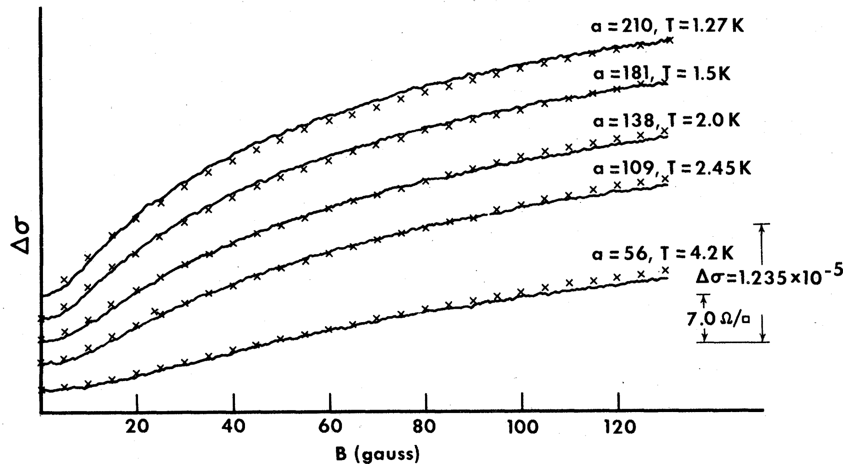

FIG. 1. Magnetoconductance as a function of magnetic field at $n_s=6.85\times10^{12}$ cm^{-2}. The conductance is 2.815×10^{-3} (ohm/ □)$^{-1}$ at 4.2 K. The solid lines are a tracing of the original data, each offset for clarity ; the $\times$'s are fits to Eq. (3) with the indicated $a=\tau_{in}/\tau_e$. At 1.27 K a 40-G magnetic field induces a $\Delta\sigma\sim\sigma_N$, which corresponds to a localization resistance caused by a decade change in temperature.

determined at various temperatures. This is illustrated in Fig. 2 for the data of Fig. 1. Following the determination of a, $\Delta\sigma$ is calculated at 5-G intervals and is indicated in Fig. 1.

The major error in the determination of τ_{in} in this procedure is due to the uncertainty in the dimensional measurements. We need to determine $D\tau_e \sim \sigma^2/n_s$, but each of these are obtained from the dimensions causing a propagating error of ~ 3 times the dimensional error. Finally $\Delta\sigma$ derived from the resistance change with field is subjected to the same dimensional error. The individual dimensional measurements have an accuracy of somewhat better than $\pm 1\%$. However, this, together with a 1% accuracy in the oxide capacitance measurement, compounds in the final determination of the absolute value of $\tau_{\text{in}} = a\tau_e$ to an uncertainty of 8%. As n_s is varied the relative values of τ_{in} are largely unaffected by this propagating error since the same dimensions are used to determine all times.

With τ_{in} determinations at fixed n_s as a function of temperature we see in Fig. 3 that $\tau_{\text{in}} \sim 1/T$. This agrees with the theoretical prediction that in two dimensions the inelastic rate due to electron-electron scattering is modified from the usual T^2

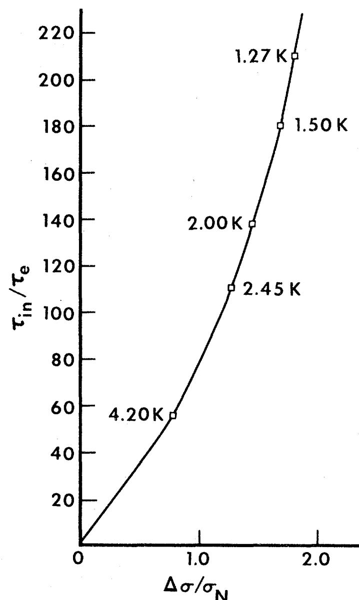

FIG. 2. Equation (3) evaluated for $D = 1.097 \times 10^{-3}$ m^2/sec, $\tau_e = 2.77 \times 10^{-13}$ sec, and $H_1 = 100$ G, corresponding to the situation of Fig. 1 as a function of $a = \tau_{\text{in}}/\tau_e$. The data points indicated are the measured values of $\Delta\sigma(H_1, T)$, hence they determine the ratio of τ_{in}/τ_e as a function of T.

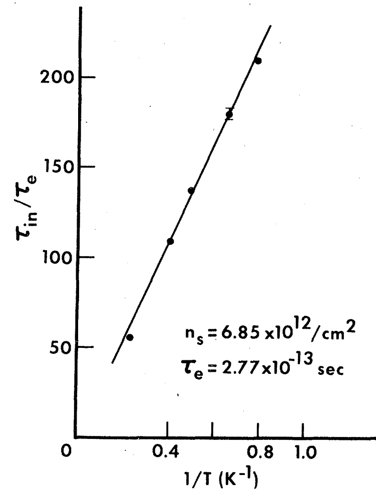

FIG. 3. τ_{in}/τ_e determined from the fit to Eq. (3) as a function of $1/T$ for $n_s = 6.85 \times 10^{12}$ cm^{-2} for device AB20. Measurement error of 10% in σ or n_s will result in fits that still produce a straight-line dependence upon $1/T$ except the intercept at $1/T = 0$ will deviate very significantly from $\tau_{\text{in}}/\tau_e = 1$, an unphysical situation.

dependence in the presence of impurities to T.[17]

The magnetoconductance measurements were made over the range of surface electron density $\sim n_s = 1 \times 10^{12}$ to $\sim 1 \times 10^{13}$. The data were analyzed for all values of n_s as described above. That is assuming a single band and thus τ_e and D are easily defined. Figure 4 shows the measured values of σ and τ_e so derived. Figures 5 and 6 show $a = \tau_{\text{in}}/\tau_e$ vs $1/T$ for all n_s values. It is worth noting that for $n_s \sim (1-2) \times 10^{12}$ cm^{-2} τ_{in} and τ_e are comparable at 4 K, while at higher densities the ratio is an order of magnitude larger. At

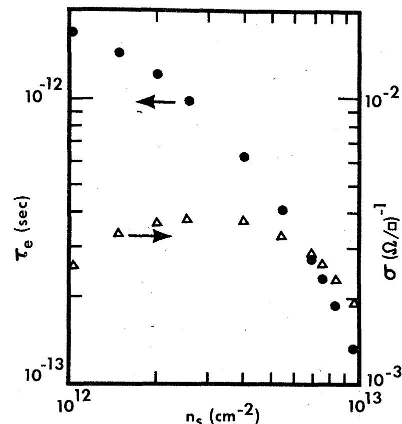

FIG. 4. The measured conductivity σ and the derived elastic scattering times as a function of n_s for device AB20. Device TB10 has almost identical characteristics.

these n_s values, the normal free-electron magnetoresistance at 100 G contributes a correction of about 10% to $\tau_{\rm in}$ at 1.27 K and corresponding larger values at higher temperatures. Since $\tau_{\rm in}$ is of the order of τ_e for these cases, the form of the theoretical expression may be in doubt. Thus all data have been analyzed without this correction. In Fig. 7 we plot $\tau_{\rm in}$ for $T=1.27$ K as a function of n_s. The striking decrease of $\tau_{\rm in}$ above $n_s \approx 7\times 10^{12}$ is suggestive of band-structure effects. It is well known that at about this surface density for [001] oriented silicon inversion layers, the next subband associated with the lighter m_z mass starts to become occupied.[18,19] Thus we need to consider these two regions, $n_s < 7\times 10^{12}$ cm^{-2} and $n_s > 7\times 10^{12}$ cm^{-2}, separately.

In the normal region of electron density ($n_s < 7\times 10^{12}$ cm^{-2}) the band model used to interpret the magnetoconductance data is well documented for [001] oriented silicon inversion layers. The justification in the sole use of

$$\sigma_N = 1.235\times 10^{-5}\ (\text{ohm}/\square)^{-1}$$

stems primarily from the theoretical prediction. However, we know that σ_N must be less than 2×10^{-5} (ohm/□)$^{-1}$ from our conductivity measurements. With this premise we have determined experimentally that the inelastic time is proportional to $1/T$. If we assume that this $1/T$ dependence continues well below 1 K and is universal in silicon MOSFET's, one may now extract from the logarithmic resistance data taken by Bishop, Tsui, and Dynes[9] the value of

$$\sigma_N \approx 1.23\times 10^{-5}\ (\text{ohm}/\square)^{-1}.$$

The data of Fig. 7 suggest that $\tau_{\rm in}$ is nearly proportional to n_s. I do not know of any theoretical treatment of such a variation.

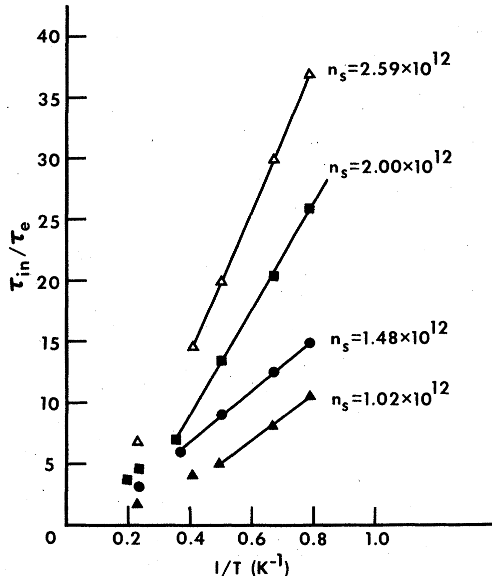

FIG. 5. $\tau_{\rm in}/\tau_e$ as a function of $1/T$ is plotted for the cases where τ_e is large, corresponding to low n_s. One observes that at high temperatures real curvature exists in some of the data which may mean that the inelastic rate has a T^2 dependence in that temperature region, although this analysis is suspect as pointed out in the body of the paper.

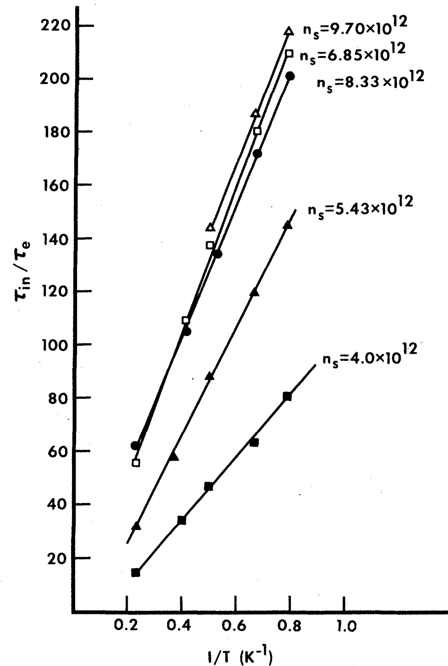

FIG. 6. $\tau_{\rm in}/\tau_e$ as a function of $1/T$ is plotted for the cases where $\tau_{\rm in}$ is much larger than τ_e corresponding to large surface charge densities.

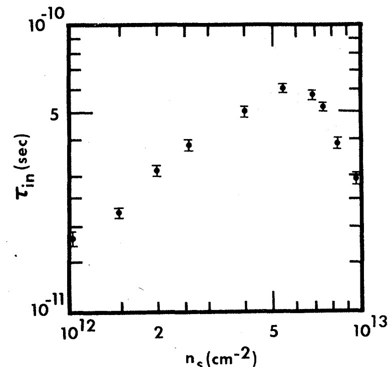

FIG. 7. The inelastic scattering times at 1.27 K obtained from data of Figs. 4 and 5 for device AB20. Device TB10 gives similar results although the falloff in inelastic time occurs at smaller n_s due to the fact that the depletion layer thickness was different with zero substrate bias.

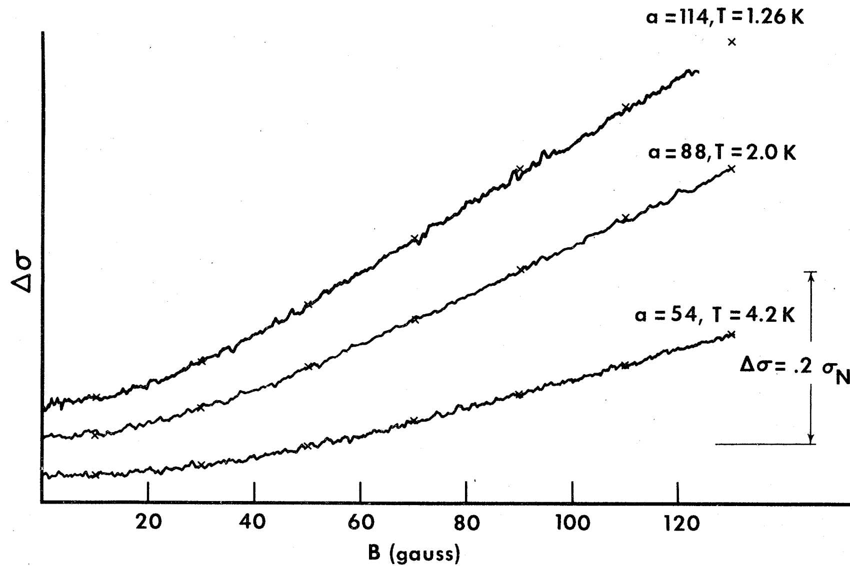

FIG. 8. Magnetoconductance of device AB20 at $n_s=1.11\times10^{13}$ cm^{-2}. In comparison with all other data the magnitude of $\Delta\sigma$ is significantly smaller. Fits using the single-band model parameters of $\sigma=1.600\times10^{-3}$ (ohm/□)$^{-1}$, $D=6.24\times10^{-3}$ m^2/sec, and $\tau_e=0.972\times10^{-13}$ sec are indicated by $\times$'s.

Concerning the anomalous region ($n_s>7\times10^{12}$ cm^{-2}) it is illustrative to examine the magnetoconductance at the high-surface charge density of $n_s=1.11\times10^{13}$ cm^{-2}. Excellent fits to the data of Fig. 8 can be obtained using D and τ_e calculated from the single-band model. Clearly such a fit is not rational since significant occupancy of six valleys is occurring.[18,19] This irrationality is further illustrated in τ_{in}/τ_e vs $1/T$ representation shown in Fig. 9.

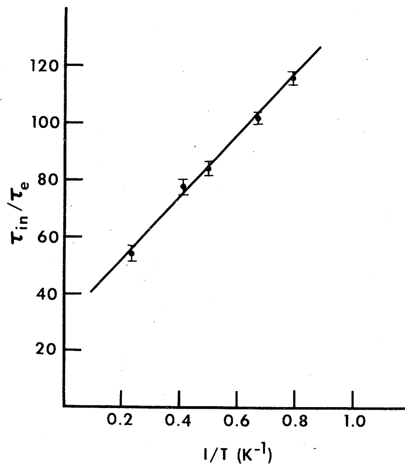

FIG. 9. $a=\tau_{in}/\tau_e$ is plotted against $1/T$ for the high-density case of Fig. 8. In contrast to all other data a very large intercept at ($1/T=0$) is indicated, a nonphysical result.

As shown by Tsui and Kaminsky,[18] as n_s is increased the subband separation continues to increase, though not as the increase in Fermi energy. One might then suppose that the initial effect is to open new inelastic scattering channels without significantly changing the elastic time, a small perturbation on the single-band model. The data suggest that with significant population of the second subband the analysis of the magnetoconductance must take this into account when deriving the diffusivity and possibly σ_N.

CONCLUSIONS

These magnetoconductance experiments have been interpreted successfully with the current theories of two-dimensional localization. The long mean free paths of the electrons in these samples lead to large magnetoconductance changes in very small fields. Inelastic lengths can now be predicted from $l_{in}=(D\tau_{in})^{1/2}$ to be of the order of 8×10^{-5} cm at 1 K. Hall experiments to confirm the localization theory need to be performed in fields where the localization resistance has not been cut off by the field. In these high-mobility samples the very small fields allowed make such an undertaking difficult. With the ability to change electron density, we have started here to use localization phenomena as a probe of the silicon-inversion-layer band structure.

ACKNOWLEDGMENTS

I am grateful for the technical assistance of Ana Codoceo and Kwang Choi, and to Atul Goel for fabricating the high-quality devices. Supported in part by the National Science Foundation Grant No. DMR-7820071 and the Office of Naval Research Grant No. N00014-76-C-1083.

APPENDIX

Equation (2.10) of Ref. 5 is written replacing $-i\Omega$ with $1/\tau_{\rm in}$:

$$\delta\sigma(H,\tau_{\rm in})=-\sigma_N \sum_{n=0}^{1/\epsilon\tau_e-1} \frac{1}{(n+\frac{1}{2})+1/\epsilon\tau_{\rm in}} .$$

Here $\epsilon=4DeH/\hbar$; where the finite sum is defined over Landau orbits n, the sum is limited to $n<n_m$. $n_m=(\hbar/2eH)(1/l^2)$ is the Landau number defined by the mean free path $l^2=2D\tau_e$. This equation may be transformed into the digamma representation using the integral representation of the digamma function [Eq. (6.3.21)] given in Abramowitz and Stegun [*Handbook of Mathematic Tables* (Washington, D.C., 1970)]. Here we obtain

$$\delta\sigma(H,\tau_{\rm in})=\sigma_N\left[\psi\left[\frac{1}{2}+\frac{1}{\epsilon\tau_{\rm in}}\right]-\psi\left[\frac{1}{2}+\frac{1}{\epsilon\tau_e}+\frac{1}{\epsilon\tau_{\rm in}}\right]\right] .$$

Normally $\tau_{\rm in}>>\tau_e$, thus replicating Eq. (1). One expects further that this equation is valid when $\omega_c\tau_e<<1$ and $\hbar\omega_c<<kT$. A question arises in the grain associated with the finite integer limit n_m-1. For small values of magnetic field no problem arises on the scale of resolution of experiment. However, for modest fields ~ 100 G and when $\tau_e\approx 10^{-12}$ sec, $\omega_c\tau_e<<1$ still applies while only a few terms appear in the sum. These lead to steps in the calculated conductivity as a function of magnetic field. Since the conductivity is experimentally a smooth variable with field, we adopt the view that since digamma functions are continuous functions of the continuous variable $1/\epsilon\tau_e$ we have an interpolation formula which may take into account thermal averaging.

---

[1]G. J. Dolan and P. Osheroff, Phys. Rev. Lett. 43, 721 (1979).

[2]P. J. Bishop, D. C. Tsui, and R. G. Dynes, Phys. Rev. Lett. 44, 1153 (1980).

[3]E. Abrahams, P. W. Anderson, D. C. Licciardello, and T. V. Ramakrishnan, Phys. Rev. Lett. 42, 673 (1979).

[4]B. L. Altshuler, A. G. Aronov, and P. A. Lee, Phys. Rev. Lett. 44, 1288 (1980).

[5]B. L. Altshuler, D. Khmel'nitzkii, A. I. Larkin, and P. P. A. Lee, Phys. Rev. B 22, 5142 (1980).

[6]S. Hikami, A. I. Larkin, and Y. Nagoka, Prog. Theor. Phys. 63, 707 (1980).

[7]P. W. Anderson, E. Abrahams, and T. V. Ramakrishnan, Phys. Rev. Lett. 43, 718 (1979).

[8]Y. Kawaguchi and S. Kawaji, J. Phys. Soc. Jpn. 48, 699 (1980).

[9]D. J. Bishop, D. C. Tsui, and R. C. Dynes, Phys. Rev. Lett. 46, 360 (1981).

[10]M. J. Uren, R. A. Davies, and M. Pepper, J. Phys. C 13, L985 (1980).

[11]R. F. Wick, J. Appl. Phys. 25, 741 (1954).

[12]J. R. Drabble and R. Wolfe, J. Electron. Control 3, 259 (1957).

[13]$\sigma_{xx}\simeq 1/\rho_{xx}(1-\omega_c^2\tau_e^2)$; at 100 G with $\tau_e=1.7\times10^{-12}$ sec, $\rho_{xx}=390$ (ohms/□), $(\omega_c\tau_e)^2=2.5\times10^{-4}$ yields a magnetoresistance of $\Delta\sigma_{xx}=-6.2\times10^{-7}$ (ohms/□)$^{-1}$. This is 5% of the measured magnetoconductance at 1.27 K.

[14]The Meissner shielding effect of the aluminum gate upon the magnetoconductance can be seen. Complete screening of the magnetic field up to 4 G is observed at 1.06 K.

[15]K. M. Cham and R. G. Wheeler, Phys. Rev. Lett. 44, 1472 (1980).

[16]F. Stern, Phys. Rev. Lett. 44, 1469 (1980).

[17]E. Abrahams, P. W. Anderson, P. A. Lee, and T. V. Ramakrishnan (unpublished; referred to in Ref. 4); A. Schmid, Z. Phys. 271, 251 (1974).

[18]D. C. Tsui and G. Kaminsky, Phys. Rev. Lett. 21, 1468 (1975); P. Stiles (private communication).

[19]F. Stern and W. E. Howard, Phys. Rev. 163, 816 (1967).